AJNR

^{31}Phosphorous and Single Voxel Proton MR Spectroscopy and Diffusion-Weighted Imaging in a Case of Star Fruit Poisoning

Y.L. Chan, H.K. Ng, C.B. Leung and D.K.W. Yeung

AJNR Am J Neuroradiol 2002, 23 (9) 1557-1560
http://www.ajnr.org/content/23/9/1557

AJNR Am J Neuroradiol 23:1557–1560, October 2002

Case Report

^{31}Phosphorous and Single Voxel Proton MR Spectroscopy and Diffusion-Weighted Imaging in a Case of Star Fruit Poisoning

Y.L. Chan, H.K. Ng, C.B. Leung, and D.K.W. Yeung

Summary: We herein describe the case of a patient with chronic renal failure complicated by star fruit poisoning. T2-weighted and diffusion-weighted MR imaging showed hyperintense lesions at the thalami and right temporo-occipital cortex. Single voxel proton MR spectroscopy revealed elevation of lactate and ^{31}phosphorous MR spectroscopy revealed elevation of inorganic phosphate and decrease of phosphocreatine and nucleoside triphosphates. The imaging and metabolic changes indicated energy deprivation, with subsequent cortical necrosis proved at autopsy.

Carambola, or star fruit, originated from Asia but has spread to many tropical countries. Outbreaks of star fruit poisoning have been reported to occur in patients with chronic renal failure who are receiving dialysis treatment after consumption of star fruit or star fruit juice in Brazil (1) and Taiwan (2). Characteristically, the patients develop hiccup, nausea, limb numbness or weakness, and then confusion. Although recovery might occur after emergent hemodialysis, death is not an infrequent outcome (2). The toxicity to these uremic patients was attributed to a neurotoxin, the nature of which has not been identified.

Case Report

The patient was a 61-year-old man with chronic renal failure undergoing continuous ambulatory peritoneal dialysis. On one occasion, he consumed six star fruits in 1 week. At the end of the week, he suddenly developed headache with hiccup and vomiting that occurred more than 10 times. He became confused the next day and was admitted for medical treatment. At admission, he had hiccup and was confused, disorientated, and unable to recognize his family members. His speech was irrelevant, and his behavior was inappropriate. The Glasgow Coma Scale score was 10/15. Pupils were sluggish. Blood pressure was 210/110 mm Hg. Lumbar puncture yielded clear CSF, with an elevated protein level (1.25 g/L) and normal glucose and cell count. Lumbar puncture was negative for herpes simplex virus, measles, mumps, and varicella. The WBC count was slightly elevated (16.5×10^9/L), and serum potassium (3.5 mmol/L), calcium (2.3 mmol/L), and ammonia (<5 μmol/L) levels were normal. EEG showed the presence of theta wave, suggestive of nonspecific encephalopathy. The results of urgent CT of the brain were normal. Acyclovir was administered, but the patient's condition deteriorated and intubation and tracheostomy were required. Hiccup and vomiting persisted, and the patient also developed clonic seizures and facial twitching.

CT performed 2 days later showed no abnormal findings. MR imaging showed hyperintense lesions in the thalami, the right hippocampus, and the cortex in the superior right temporo-occipital lobe junction (Fig 1A), together with a few small cortical lesions scattered in the rest of the cerebral hemispheres on T2-weighted images. On T1-weighted images, subtle and slightly hypointense change was observed at the thalami and right superior temporo-occipital junction (Fig 1B). On diffusion-weighted images, both cortical and thalamic lesions were conspicuously more hyperintense than on T2-weighted images (Fig 1C) and lesion was also detected in the tegmentum. There was no associated mass effect or enhancement after IV administered contrast material.

Single voxel proton MR spectroscopy of the right temporo-occipital lobe lesion showed decreased *N*-acetylaspartate concentration and the presence of lactate (Fig 1D). ^{31}Phosphorous MR spectroscopic imaging showed decreased phosphocreatine and β-nucleoside triphosphates and elevated inorganic phosphate in the $3 \times 3 \times 3$ cm^3 voxels encompassing each thalami and right temporo-occipital junction (Fig 1E).

Hemodialysis was administered, and improvement in the patient's general condition was achieved. A second MR imaging examination performed 3 weeks later showed the persistence of hyperintense lesions on T2-weighted images. The cortical and thalamic lesions became hyperintense on T1-weighted images (Fig 2A). Although lactate persisted in the right temporo-occipital lesion on single voxel proton MR spectroscopy, signs of energy deprivation were no longer evident on ^{31}phosphorous MR spectroscopic imaging (Fig 2B). However, no neurologic recovery was achieved. The Glasgow Coma Scale score dropped to 3/15, and the patient remained confused and then died during the 7th week after admission.

An autopsy examination showed laminar necrosis in the right temporal lobe and occipital lobe. There was liquefactive necrosis affecting the deeper layers of the cortical ribbon with capillary proliferation. The adjacent areas showed cell loss and florid gliosis. The thalami and tegmentum showed diffuse cell loss and gliosis but no liquefaction. No encephalitis or infective focus was identified. No vascular occlusion of the basilar artery or arteries of the circle of Willis or their branches occurred as far as anatomic dissection was feasible. Multiple tissue samplings of the cerebrum did not show thrombus, embolus, or vasculitis.

Discussion

Chang et al (2) reported star fruit poisoning in 20 patients undergoing dialysis, eight of whom died. CT

Received December 18, 2001; accepted after revision March 19, 2002.

From the Departments of Diagnostic Radiology and Organ Imaging (Y.L.C.), Anatomical and Cellular Pathology (H.K.N.), Medicine and Therapeutics (C.B.L.), and Clinical Oncology (D.K.W.Y.), Prince of Wales Hospital, The Chinese University of Hong Kong, Hong Kong.

Address reprint requests to Y.L. Chan, Department of Diagnostic Radiology & Organ Imaging, Prince of Wales Hospital, Shatin, N.T., Hong Kong.

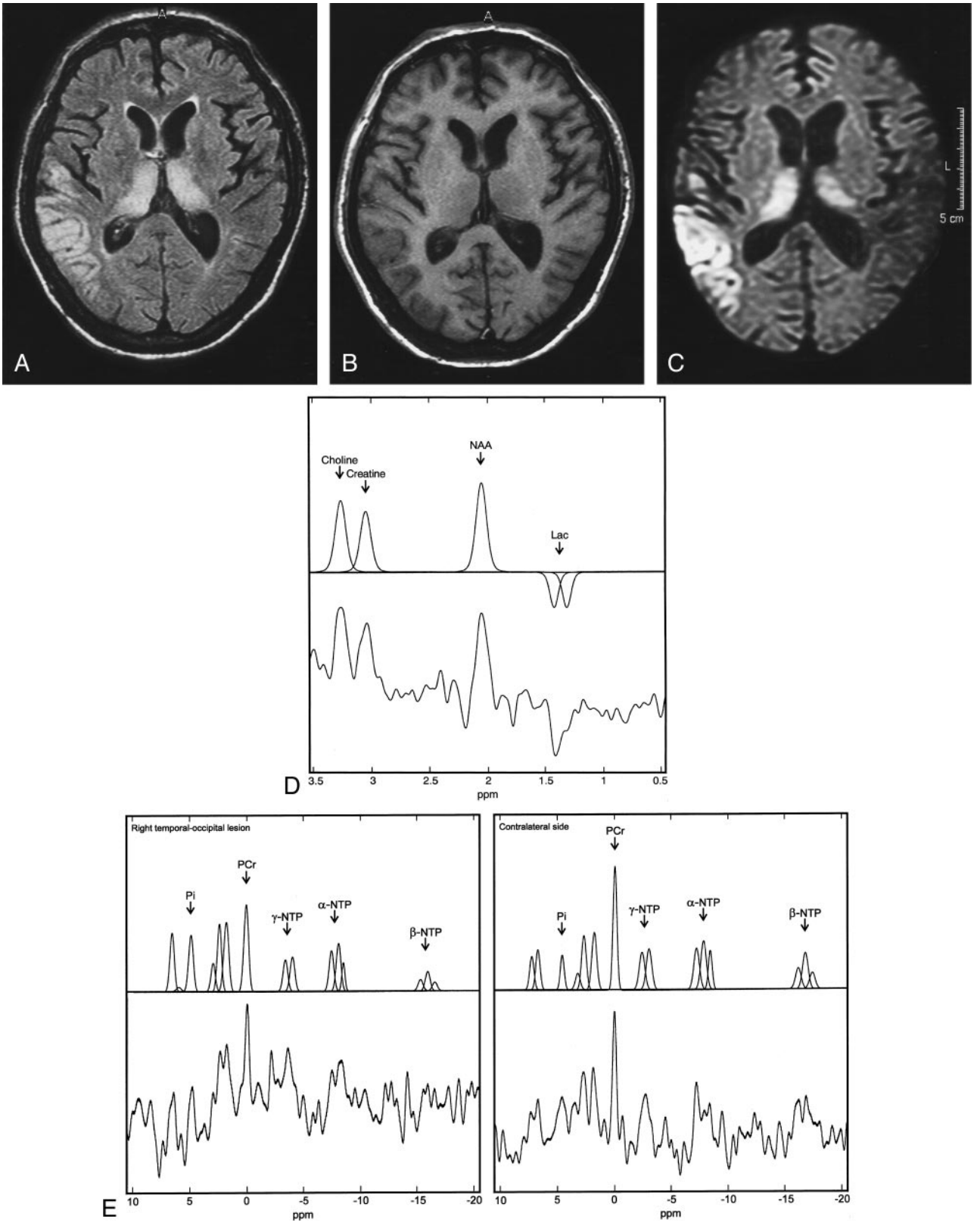

FIG 1. MR images and MR spectroscopy obtained 3 days after admission.

A, Axial view fluid-attenuated inversion recovery T2-weighted MR image (8000/110/1 [TR/TE/NEX]; inversion time, 2400 ms) shows symmetrical hyperintense lesions in both thalami. In the right temporo-occipital lobe junction, gyriform hyperintensity is observed.

B, Axial view T1-weighted MR image (500/15/2) shows a subtle decrease in signal intensity in the thalami and the right superior temporo-occipital junction.

C, Axial view diffusion-weighted image (b = 800 s/mm^2; 1600/22/2; diffusion TE, 80 ms) shows the hyperintense lesion in the thalami and right superior temporo-occipital lobe junction in a more conspicuous manner than does the T2-weighted MR image (compare with *panel A*).

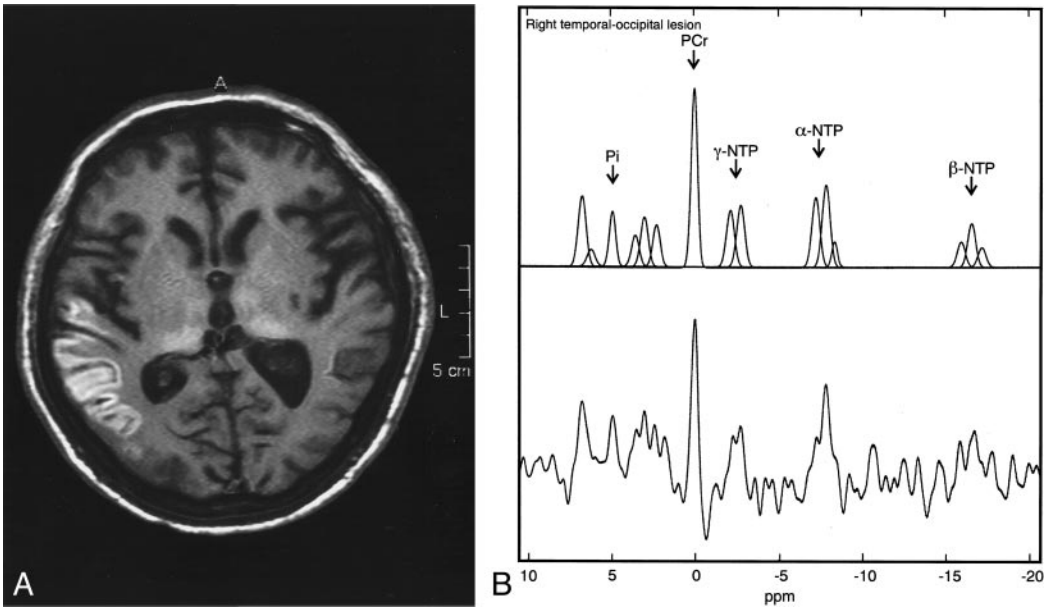

FIG 2. MR images and ^{31}phosphorous MR spectrum obtained 4 weeks after admission and after hemodialysis.
A, Axial view T1-weighted MR image shows hyperintense change at the thalami and right superior temporo-occipital lobe cortex.
B, ^{31}Phosphorous MR spectrum shows phosphocreatine (*PCr*). β-nucleoside triphosphates (*β-NTP*), relative to inorganic phosphate (*Pi*) in the right temporo-occipital lobe (same voxel as that shown in Fig 1, *panel E*), have increased to reach normal levels.

was performed for 10 of these 20 patients, and in none was there evidence of organic lesions. The two CT studies performed for our patient also revealed no morphologic lesion. The MR imaging features associated with star fruit poisoning have not been reported in the literature. T2-weighted images of the brain of our patient showed hyperintense lesions in the gray matter of cerebral hemispheres and both thalami. On T1-weighted images, the cortical lesions changed from being mildly hypointense to hyperintense in a time course of 3 weeks. The hyperintense changes resemble the cortical laminar hyperintensity on T1-weighted images reported in cerebral infarcts 2 weeks after ictus, which was shown not to be due to hemorrhagic infarction (3).

The cerebral cortical and thalamic lesions were more markedly hyperintense on the diffusion-weighted images than on the T2-weighted images, which suggests restricted diffusion. Acute ischemic infarction is the most frequently encountered lesion with restricted diffusion. Linked to a breakdown in energy metabolism (4), shift of extracellular to intracellular water, reduction of intracellular water motion (5), and tortuosity of extracellular space (6) have been suggested to contribute to the restriction in diffusion. Other acute neurologic diseases manifesting as hyperintense lesions on diffusion-weighted images include encephalitis due to herpes simplex and influenza virus (7), global cerebral anoxia due to prolonged cardiac arrest (8), diffuse axonal injury (9), fluoroacetamide intoxication (10), and variant Creutzfeldt-Jakob disease (11). Among these entities, only variant Creutzfeldt-Jakob disease characteristically shows thalamic hyperintense change on diffusion-weighted images (11).

The clinical presentation and course of our patient were different from the aforementioned diseases. There was also no histologic evidence of encephalitis, vascular occlusion, or spongiform encephalopathy. Hyperintense lesions may be found in white matter and cortex on T2-weighted images in hypertensive encephalopathy, but unlike lesions found in our patient, they are characteristically reversible and do not show bright signal intensity on diffusion-weighted images.

An autopsy of our patient showed laminar necrosis of the cortex in the involved brain tissue. Cortical laminar necrosis has been observed in brains of rats subjected to four-vessel occlusion and has been documented in patients with cardiac arrest (8). Diffuse cerebral cortical laminar necrosis mediated by neurotoxin has also been shown in cattle with acute hydrogen sulfide (pit gas) poisoning (12).

MR spectroscopy of the current patient also supported a breakdown in energy metabolism as the underlying pathophysiological process. The decrease

FIG. 1. *Continued*
D, Single voxel proton MR spectrum (2000/136) shows a decreased *N*-acetylaspartate (*NAA*) peak at 2.02 ppm in the right temporo-occipital lobe lesion. Lactate (*Lac*) is shown with the inverted doublet centered around 1.33 ppm. Unprocessed and processed spectra are shown, respectively, on the lower and upper parts of the figure.
E, ^{31}Phosphorous MR spectrum shows decreased phosphocreatine (*PCr*) at 0 ppm, β-nucleotide triphosphate (*β-NTP*) at −16.3 ppm, and elevated inorganic phosphate (*Pi*) at 4.9 ppm in the right temporo-occipital lobe lesion compared with the contralateral morphologically intact left side. Unprocessed and processed spectra are shown, respectively, on the lower and upper parts of the figure.

in *N*-acetylaspartate on proton MR spectroscopy indicates neuronal loss or dysfunction and the presence of lactate indicates anaerobic glycolysis as a result of interference of the normal cellular oxidative respiration. ^{31}Phosphorous MR spectroscopic imaging of the lesion sites at the right temporo-occipital junction and thalami showed decreased phosphocreatine and nucleoside triphosphates (represented by β-nucleoside triphosphates as resonances of nucleoside diphosphates overlapped with γ- and α-nucleoside triphosphates) and elevation of inorganic phosphate. These changes indicate energy deprivation at the cellular level. A reduced phosphocreatine with elevated inorganic phosphate andadenosine 5′-diphosphate has been observed in both muscle and brain on ^{31}phosphorous MR spectroscopy of a patient with MELAS syndrome (mitochondrial myopathy, encephalopathy, lactic acidosis, and recurrent stroke-like episodes) with hypoattenuated lesions in bilateral parietooccipital lobes on CT scans (13). Mitochondrial disorders may have features of hyperintense lesions involving the thalami and cerebral white matter on T2-weighted images (14) that may be diagnostically confused with the imaging findings in our case except for the different clinical presentations. The alleged star fruit neurotoxin, accumulating to toxic levels because of failure of elimination in uremic patients, probably acts by interfering with oxidative phosphorylation in the mitochondrion with depletion of adenosine triphosphate, leading to cell dysfunction and death. The preferential involvement of deep gray matter of the thalami and the cortical ribbon might be explained by the higher sensitivity to energy deprivation in neurons. It has been shown that the rate of reduction in diffusion is greater in the gray than it is in the white matter during ischemia and after cardiac arrest in animal models (6).

The toxic substance responsible for star fruit poisoning in uremic patients has not been identified but is thought to be a water-soluble excitatory neurotoxin. Neto et al (1) injected star fruit extract into the peritoneal cavity and cerebral ventricles of mice and rats and observed tonicoclonic convulsions in these animals. Considering that five of six of their patients recovered after hemodialysis, they suggested that the toxic substance is a water-soluble excitatory neurotoxin, which can be removed by hemodialysis. The improvement of energy deprivation shown by the second ^{31}phosphorous MR spectroscopy study of the patient, performed after hemodialysis, seems to support the suggestion of a toxin removable by hemodialysis. Excitotoxic injury has been shown to be associated with restriction in diffusion at the time of intrastriatal injection of *N*-methyl-D-aspartate, a glutamate agonist, into rat brains (5). A significant change of metabolite levels, as assessed by proton MR spectroscopy, was not observed in these animals during the first hours, but complete loss of brain metabolites was observed at 72 hours, probably as a result of delayed neuronal death.

Conclusion

The elevation of inorganic phosphate and reduced phosphocreatine and nucleoside triphosphates and elevation of lactate on ^{31}phosphorous and proton MR spectra and hyperintense change on diffusion-weighted images in this case of star fruit poisoning indicate a neurotoxin that interferes with oxidative phosphorylation. Because the neurons are susceptible to this process of energy depletion at the cellular level, they exhibit intra- and extracellular changes from which restriction in diffusion and finally cortical necrosis ensue.

References

1. Neto MM, Robl F, Netto JC. **Intoxication by star fruit (*Averrhoa carambola*) in six dialysis patients?** *Nephrol Dial Transplant* 1998; 13:570–572
2. Chang JM, Hwang SJ, Kuo HT, et al. **Fatal outcome after ingestion of star fruit (*Averrhoa carambola*) in uremic patients.** *Am J Kidney Dis* 2000;35:189–193
3. Komiyama M, Nakajima H, Nishikawa M, Yasui T. **Serial MR observation of cortical laminar necrosis caused by brain infarction.** *Neuroradiology* 1998;40:771–777
4. Pierpaoli C, Alger JR, Righini A, et al. **High temporal resolution diffusion MRI of global cerebral ischemia and reperfusion.** *J Cereb Blood Flow Metab* 1996;16:892–905
5. Dijkhuizen RM, de Graaf RA, Tulleken KA, Nicolay K. **Changes in the diffusion of water and intracellular metabolites after excitotoxic injury and global ischemia in neonatal rat brain.** *J Cereb Blood Flow Metab* 1999;19:341–349
6. Norris DG, Niendorf T, Leibfritz D. **Health and infarcted brain tissues studied at short diffusion times: the origins of apparent restriction and the reduction in apparent diffusion coefficient.** *NMR Biomed* 1994;7:304–310
7. Tsuchiya K, Katase S, Yoshino A, Hachiya J. **Diffusion-weighted MR imaging of encephalitis.** *AJR Am J Roentgenol* 1999;173;1097–1099
8. Arbelaez A, Castillo M, Mukherji SK. **Diffusion-weighted MR imaging of global cerebral anoxia.** *AJNR Am J Neuroradiol* 1999;20: 999–1007
9. Takayama H, Kobayashi M, Sugishita M, Mihara B. **Diffusion-weighted imaging demonstrates transient cytotoxic edema involving the corpus callosum in a patient with diffuse brain injury.** *Clin Neurol Neurosurg* 2000;102:135–139
10. Huang L, Liu SR, Cao G. **Diffusion in acute intoxicated human brain.** Proceedings of 9th Annual Scientific Meeting of the International Society for Magnetic Resonance in Medicine. Glasgow, 2001
11. Collie DA, Sellar RJ, Zeidler M, Colchester AC, Knight R, Will RG. **MRI of Creutzfeldt-Jakob disease: imaging features and recommended MRI protocol.** *Clin Radiol* 2001;56:726–739
12. Hooser SB, Van Alstine W, Kiupel M, Sojka J. **Acute pit gas (hydrogen sulfide) poisoning in confinement cattle.** *J Vet Diagn Invest* 2000;12:272–275
13. Hayes DJ, Hilton-Jones D, Arnold DL, et al. **A mitochondrial encephalopathy: a combined ^{31}P magnetic resonance and biochemical investigation.** *J Neurol Sci* 1985;71:105–118
14. Valanne L, Ketonen L, Majander A, Suomalainen A, Pihko H. **Neuroradiologic findings in children with mitochondrial disorders.** *AJNR Am J Neuroradiol* 1998;19:369–377